Exploring the optical and dielectric properties of bifunctional and trifunctional epoxy polymers

Haythem Jdidi [a,b], Najla Fourati [b], Chouki Zerrouki [b,*], Laurent Ibos [c], Magali Fois [c], Alain Guinault [d], Wissal Jilani [a,e], Samir Guermazi [a], Hajer Guermazi [a,**]

[a] Physics of Insulators and Semi-insulator Materials Research Unit, Faculty of Sciences of Sfax, Sfax University Tunisia, B.P: 1171, 3038, Tunisia
[b] SATIE, UMR 8029, CNRS, ENS Paris-Saclay, Cnam, 292 Rue Saint-Martin, 75003, Paris, France
[c] CERTES/OSU Efluve, Paris-Est Créteil University, 61 Avenue du Général de Gaulle, 94010, Créteil, France
[d] PIMM, UMR 8006, Arts et Métiers ParisTech, CNRS, Cnam, 151 Bd de L'Hôpital, F-75013, Paris Cedex, France
[e] Department of Physics, Faculty of Sciences and Arts Dhahran Al Janoub, King Khalid University, P.O. Box 9004, Abha, 61421, Saudi Arabia

A B S T R A C T

Two polymers were prepared from diglycidyl ether of bisphenol A (DGEBA) and triglycidyl *p*-aminophenol (TGAP) epoxy resins, using the same hardener diethylenetriamine (DETA). The obtained polymers were compared in terms of structural, optical, mechanical, thermal and dielectric properties. Dielectric spectroscopy and dynamic mechanical analysis indicated the presence of dipolar dielectric relaxations in both polymers, and interfacial one only for TGAP/DETA, which is consistent with XRD findings. Different approaches were considered to fit electrical modulus and conductivity and to estimate the relaxation times and activation energies according to temperature. For optical measures, a novel result processing approach is proposed for an accurate determination of the polymers bandgap and for highlighting the existence of additional energy transition level for TGAP. Results indicate that this polymer could be a potential candidate for use as a protective film and as UV/blue-light filter for screens and windows.

1. Introduction

Epoxy resins are an important class of versatile thermosetting systems, classified as high-performance materials, thanks to their high strength, low creep, low cure shrinkage, excellent resistance to corrosion, good adhesion to many substrates, an appropriate mechanical, thermal and opto-electrical characteristics [1]. Epoxy-based polymers are used in a wide variety of applications such as adhesives, high-performance composites, coatings, electronic encapsulation, electrical components and aerospace [2–7]. The main advantage of epoxy resins is the possibility of crosslinking with the reactive functional groups of the polyamine hardener without releasing volatile products. The number of epoxy and amine reactive groups are the key elements that drive the properties of epoxy polymers. A judicious choice of an epoxy monomer and the further curing agent permits thus to obtain highly crosslinked epoxy thermosets with outstanding physico-chemical properties [8–11]. Other parameters like the preparation conditions, the duration and the temperature of curing are of prime importance in the network structure of a given epoxy based polymer [12–15]. Several studies were devoted to the comparison of optical, thermic, and mechanical properties of epoxy polymers. Some of them reported the use of the same hardener and different epoxy resins, while other ones have used the same epoxy resin and investigated several hardeners [16–29].

The objective of this study is to investigate the effect of the number of epoxy functional groups on the structural, optical, dynamic mechanical, thermal and dielectric behaviors of epoxy based polymers. We have thus chosen to investigate a bifunctional, diglycidyl ether of bisphenol A (DGEBA), and a trifunctional, triglycidyl *p*-Aminophenol (TGAP) polyepoxyde resins, and we have cured them with the same hardner: diethylenetriamine (DETA). Compared to other studies devoted to the comparison of the physico-chemical properties of DGEBA/DETA and TGAP/DETA polymers, here we focused on neat polymers without additional fillers (clays, carbon nanotubes, silicates, graphite ….).

The optical properties of the polymers were determined from transmittance and absorbance spectra, mainly in terms of optical bandgap (E_g), usually estimated from the empiric Tauc equation (eq.

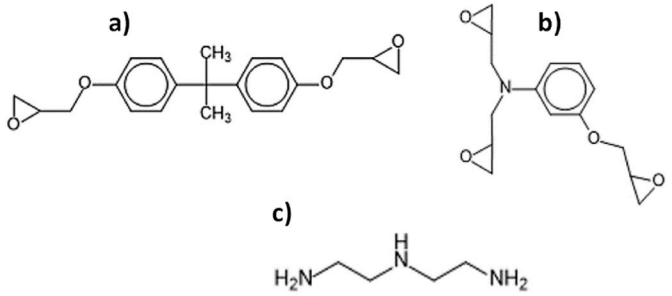

Fig. 1. Chemical structures of (**a**) diglycidyl ether of bisphenol A (DGEBA), (**b**) Triglycidyl *p*-Aminophenol (TGAP) and (**c**) diethylenetriamine (DETA).

(1)) [30].

$$\alpha h\upsilon = A\left(h\upsilon - E_g\right)^n \tag{1}$$

Where A is a constant, $h\upsilon$ is the incident photon energy, α is the optical absorption coefficient determined from absorbance data and n is an exponent characteristic of the optical transition. The factor n is close to 1/2 for the direct allowed transition, and to 2 for the indirect one. The optical bandgap energy can thus be estimated from the linear part of $(\alpha h\nu)^2$ variation versus photon energy ($h\nu$) for the direct transition and from that of $(\alpha h\nu)^{0.5}$ for the indirect one. The classical use of this model, which is very useful for the experimental determination of the Eg value, remains nevertheless "relatively limited" regarding the rational distinction of the nature of the transition, direct or indirect. Knowing the type of the transition is in fact of prime importance, as it greatly conditions the optoelectronic properties of a given material, and therefore its possible applications. Some publications reported the estimated values of the two gaps via the Kubelka-Munk function and determined the nature of transition only by calculation [31,32]. Other works have rightly underlined this difficulty of defining the transition type and made proposals to remove this ambiguity by using the R-squared value to estimate the goodness of the fit of Tauc plots [33]. Others proposed an algorithm for automated Tauc-plot analysis [34], or a modified Tauc-Lorentz dispersion model [35].

In this work, we propose a novel approach of results processing, based on the logarithmic derivative of Tauc's law which would permit to estimate more accurately the Eg value and to better account for the nature of the transition in DGEBA/DETA and TGAP/DETA polymers.

The relaxation temperatures of these cured systems were estimated using two complementary techniques: dynamic mechanical thermal analysis and impedance spectrometry. The further relaxation times and activation energies were estimated and compared.

Polymers structural and chemical identifications were probed by X-ray diffractometry and Fourier-Transform Infrared spectrometry.

The aim of all these measurements was to show that increasing the number of epoxy functions in a given prepolymer, leads to a considerable change in all the properties of the considered polymer, thus enlarging the field of application of this type of material.

2. Experimental

2.1. Materials and preparation

Diglycidyl ether of bisphenol-A epoxy (DGEBA), triglycidyl *p*-Aminophenol (TGAP), and diethylenetriamine (DETA) were purchased from Sigma Aldrich. Their chemical structures are shown in Fig. 1.

The polymers were prepared as follows: each epoxy resin was first sonicated through uring 1 h, to minimize the presence of air bubbles prior to the addition of DETA hardener, in a molar ratio 1/1. The preparation was then thoroughly stirred at 600 rpm during 2 min for DGEBA/DETA and during 10 min for TGAP/DETA, then placed in an ultrasonic bath for 10 min, to homogenize the mixture and to remove air bubbles, and then put in 4 cm diameter silicone molds.

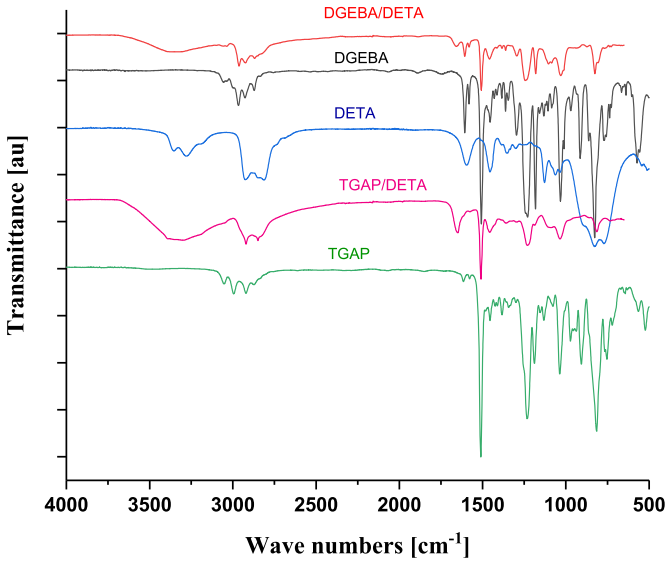

Fig. 2. FTIR spectra of the DETA hardener, DGEBA and TGAP resins, and the DGBA/DETA and TGAP/DETA polymers.

DGEBA/DETA blends were cured at 60 °C during 2 h, then at 120 °C for 2 h, and finally post-cured at 140 °C for 1 h. TGAP/DETA blends were first cured during 1 h at 60 °C, then 1 h at 100 °C, 2 h at 150 °C, and finally post-cured 1 h at 170 °C. All the temperatures and durations were optimized to obtain reproducible and well crosslinked disc-shaped samples with a thickness of about 1.5 mm (results not shown here).

2.2. Characterization techniques

Differential scanning calorimetry (DSC) measurements were performed with a Pyris PerkinElmer thermal analyzer. An empty aluminum pan was used as the reference, and the instrument was calibrated with indium. Each sample was placed in the DSC chamber, pre-set at 30 °C, and then heated till 190 °C with a linear heating rate of 10 °C/min.

Fourier transform infra-red (FTIR) analysis were carried out with a PerkinElmer spectrometer.

The spectra were recorded in the transmission mode in the range from 650 to 4000 cm^{-1} with a resolution of 2 cm^{-1}. A background spectrum was recorded before each measurement, and the further "background corrections" were systematically operated.

An X-ray diffractometer (XRD) (D8-Advance Bruker), working in Bragg-Brentano geometry with CuK_α radiation (λ = 1.54056 Å), was used for polymers structural characterization.

The absorbance and the transmittance of the polymers were analyzed using a Lambda 750S UV–VIS–NIR spectrophotometer (PerkinElmer) in the wavelength range of 200–860 nm.

Thermal stability analyses were carried out with a TGA 4000 thermogravimetric analyzer (PerkinElmer). The measurements were performed at a heating rate of 2 °C/min from room temperature to 600 °C.

Thermo-mechanical measurements were carried out with a Tritec 2000 dynamic mechanical temperature analyzer at a frequency of 1 Hz and a displacement of 0.05 mm. DGEBA/DETA and TGAP/DETA polymers were heated from 30 to 200 °C at a heating rate of 2 °C/min. Measurements were done in the 3 points bending configuration. The glass transition temperature of each polymer was estimated from the peak value in the tan δ plot.

Dielectric measurements were performed using a Solartron analytical impedance spectrometer, at the frequency interval of 0.1–1 MHz and a temperature range from −100 to 200 °C.

Notice that the time between the realization of the samples and their analysis did not exceed one week for XRD, UV–Vis, DSC, DMTA and

Table 1
Characteristic bands of DGEBA and HDGEBA in the mid IR.

	Wavenumber (cm^{-1})	Functional groups
DGEBA	3050	C–H tension of the methylene group of the epoxy ring
	2967	StretchingC-H of CH2
	2927	Stretching C–H of aromatic and aliphatic
	2873	CH stretching vibrations
	1607	Stretching C═C of aromatic rings
	1508	Symmetric vibration C═C, aromatic
	1457	Symmetric vibration C═C, aromatic
	1183	C–O aromatic ring stretching
	1034	Stretching C–*O*–C of ethers
	914	Stretching C–O of oxirane group
	828	Stretching C–*O*–C of oxirane group
	3050	C–H tension of the methylene group of the epoxy ring
	2927–3000	NH2 (primary amine)
	1513	Aromatic ring
	1227	OH (hydroxyl, ether)
TGAP	1038	Stretching C–*O*–C of ethers
	912	Stretching C–O of oxirane group
	813	Stretching C–*O*–C of oxirane group
	3364	N–H stretching vibration
	2930	Asym. C–H stretch stretching vibration
	2810	Symmetric CH_2 stretching vibration
	1601	NH deformation vibration
DETA	1462	CH deformation
	1130	C–N stretching vibration

dielectric spectroscopy measurements. Whereas, for Thermogravimetric analysis and FTIR spectroscopy, the storage time was 6 months for TGAP and 3 months for DGEBA. During these storage periods, the samples were stored in individual plastic bags with a zipper closure, all of which were placed in a closed tinted glass bottle. Under these storage conditions, the samples are relatively protected from UV light, and a limited effect of air and moisture can be expected.

3. Results and discussion

3.1. Structural characterization

3.1.1. Fourier transform infra-red spectroscopy

FTIR spectra of the DETA hardener, DGEBA and TGAP resins, and further DGEBA/DETA and TGAP/DETA polymers are presented in Fig. 2.

DGEBA and TGAP bands were assigned in Table 1, according to literature [23,36–41].

Compared to DGEBA and TGAP spectra, those of DGEBA/DETA and TGAP/DETA polymers exhibit two new bands: i) broad absorption bands around 3355 cm^{-1} (for DGEBA/DETA) and 3330 cm^{-1} (for TGAP/DETA) which can be assigned to the stretching vibration modes of OH and NH groups, and ii) bands at 1130 cm^{-1} which can be attributed to the υ(C–N) stretching vibration.

FTIR spectra highlight also the disappearance of the two characteristic bands of the oxirane ring epoxy rings: *i)* that of C–O deformation of the oxirane group (centered at 915 cm^{-1} in DGEBA and at 912 cm^{-1} in TGAP) and *ii)* the weak peak (centered at 3050 cm^{-1}) attributed to C–H tension of the methylene group of the epoxy ring. This result confirms that the crosslinking process has taken place.

3.1.2. DSC characterization

DSC thermograms of DGEBA/DETA and TGAP/DETA are plotted in Fig. 3. Here, we have chosen to present only the first and second heating cycles. Fig. 3 shows that the thermal behavior of the two polymers is not the same. Indeed, in the case of DGEBA, we observe a first cycle with two peaks, which would indicate that the polymerization is probably not finished. The second cycle allows to "erase this "memory", and we find the classical thermogram of a DGEBA/amine. In the case of TGAP/EDTA, the thermograms of the two cycles are almost comparable, which would indicate that the polymeric network was formed rather quickly, due to the greater number of epoxy groups.

3.1.3. X-ray diffraction

X-ray diffraction (XRD) measurements were carried out to highlight

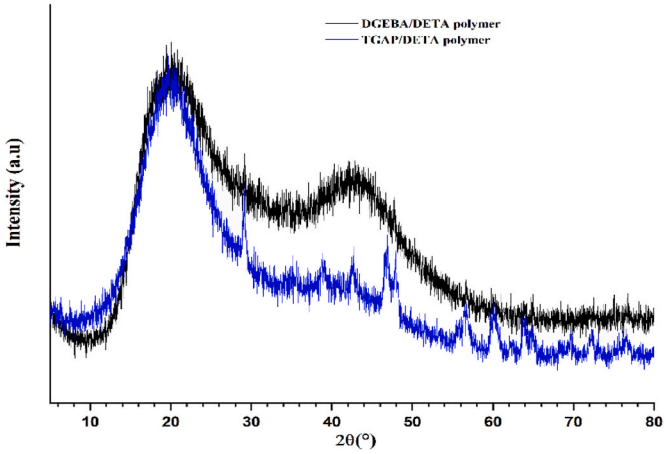

Fig. 4. XRD diffractograms of the DGEBA/DETA and TGAP/DETA polymers.

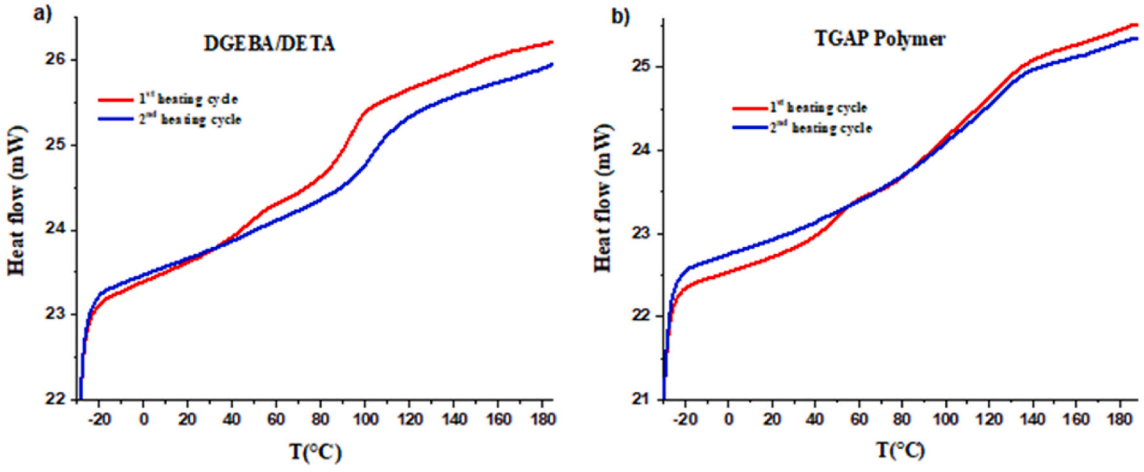

Fig. 3. DSC thermograms of DGEBA/DETA and TGAP/DETA. Only the heating cycles are presented.

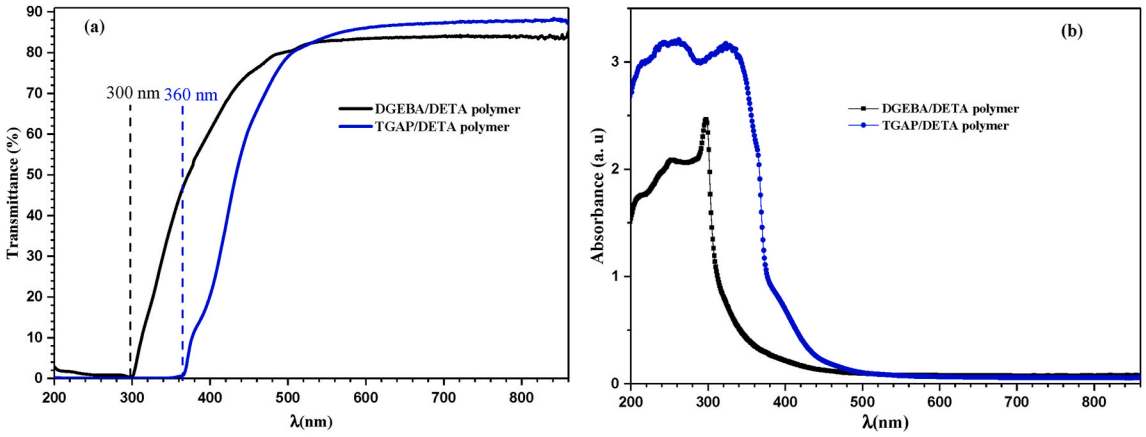

Fig. 5. Transmittance (**a**) and Absorbance (**b**) spectra of the DGEBA/DETA and TGAP/DETA polymers.

the role of the number of epoxy functions on the structural properties of DGEBA/DETA and TGAP/DETA polymers. The obtained XRD patterns (Fig. 4) showed a broad peak observed around $2\theta = 20°$ for both polymers, indicating their amorphous nature.

The XRD diffractogram of TGAP sample reveals, however, the existence of some narrow peaks that overlap the scattered reflection. These peaks indicate the existence of oriented microdomains in the amorphous polymeric matrix. The doubling of some peaks seems indicate a "twin" structure, but the scattering preponderant effect makes the measurements relatively noisy. Nevertheless, we have estimated the mean periodicity of these structures at (0.59 ± 0.02) nm. These nanostructures are probably due to the molecular chains stacking as already observed in our previous work [28]. As this difference between the two polymers' structures may lead to disparities in their properties, we have investigated several other characterization methods.

3.2. *Optical properties*

Fig. 5 illustrates the optical responses of both polymers. The transmittance spectra, presented in Fig. 5a, show that the main difference between the realized polymers is related to the wavelength cut-off, of about 300 nm for DGEBA/DETA and of order of 360 nm for TGAP/DETA. Beyond 500 nm, the transmittance is relatively comparable for both polymers, which exhibit a transparency higher than 80%.

The absorbance spectra presented in Fig. 5b reveal high absorption level in the UV region. Some absorption peaks are observed in the region 242–262 nm and around 323 nm for TGAP/DETA, and around 252 and 297 nm for DGEBA/DETA. These peaks are mainly due to n-π^* and π-π^* electronic transitions [42–46].

In fact, yellowing has often been observed on epoxy-based polymers. Some authors have assigned this phenomenon to a combination of causes, the most important of which is the thermo-oxidative formation of carbonyls during curing [47]. In our case, even if an oxidation may exist for the TGAP samples, it is not preponderant. The presence of parts relatively structured into the amorphous matrix, is the main cause of the observed shift on transmittance/absorbance spectra. These very localized structures can result from molecular chains stacking, which gave rise to the diffraction spectrum superimposed on a diffuse background (XRD measurements), and to singularities in absorbance spectrum due to electronic transitions, that are more resolved in TGAP than DGEBA. This should be confirmed by dielectric spectroscopy measurements with a possible presence of interfacial relaxation, only for TGAP.

At this stage, the main difference between the two polymers concerns the UV-blocking character. Indeed, at 380 nm (the U–V/violet limit) the TGAP/DETA transmittance is of 12%, while it is about 54% for the DGEBA/DETA. At 430 nm (violet-indigo limit), the transmittance drops by only 16% for DGEBA/DETA compared to its value at 600 nm, while it is almost halved (46%) for TGAP/DETA. Due to its interesting transmittance properties, TGAP/DETA could be used in several applications, such as UV and blue radiations filter.

These measures can also permit to determine the optical bandgap energy E_g of the two considered polymers from the Tauc equation (eq. (1)).

In our case, we plotted, for both polymers, $(\alpha h\nu)^2$ and $(\alpha h\nu)^{0.5}$ variations versus photon energy ($h\nu$) to choose only the one which presents a region that can be linearly fitted with the lowest associated

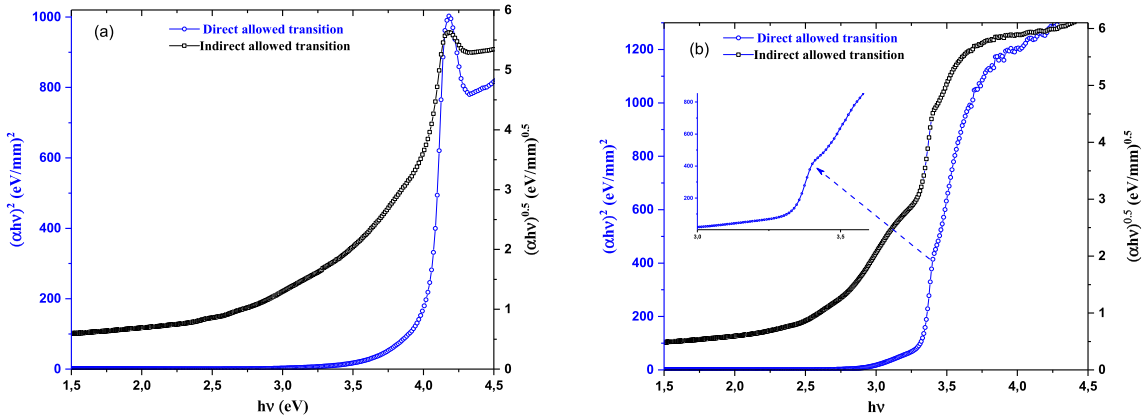

Fig. 6. Tauc's plots for direct and indirect bandgap, for (a) DGEBA/DETA and (b) TGAP/DETA. The inset shows a slope change between two linear parts for TGAP/DETA.

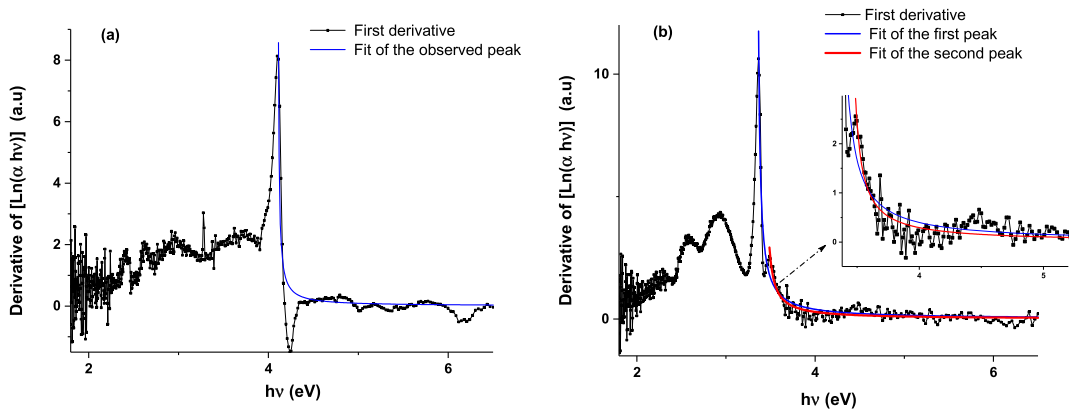

Fig. 7. Derivatives of Ln (αhν) versus (hν) for (a) DGEBA/DETA and (b) TGAP/DETA and the further corresponding fits for energies superior to Eg values. The inset shows the second peak.

uncertainties. The corresponding spectra are reported on Fig. 6.

Fig. 5a shows that although the two plots for DGEBA/DETA polymer present linear regions, the direct allowed transition seems to be more appropriate. The choice is however less obvious for the TGAP/DETA polymer, as we observe two quasi-linear zones for each representation.

This peculiarity appears to tilt the choice towards an indirect transition. Moreover, in the hypothesis of a direct transition, the extrapolation of the linear zone located at high energies intercepts the x-axis at a lower value (3,28 eV) than that obtained by extrapolation of the linear zone (3,32 eV) at low energies.

The difficulty of discriminating the transition type (direct/indirect) could be attributed to a relatively small shift, between the position of the maximum of the valence band and that of the minimum of the conduction band, in the wave-vector space.

To confirm the hypothesis of indirect transition, let us recall that the Tauc's relation (eq. (1)) takes into account only the band-to-band absorption, and that the range where its validity is assumed, is too small to be sure of the exact value of the exponent n [30]. We have therefore chosen to operate mathematical treatments for the Tauc equation, by first transforming it in a logarithm form (eq. (2)) and then by differentiating the obtained result (eq. (3)). Notice that it is possible to apply the logarithm to eq. (1) since its both members have positive and not zero values.

$$Ln(\alpha h\upsilon) = Ln(A) + n \times Ln\left(h\upsilon - E_g\right) \tag{2}$$

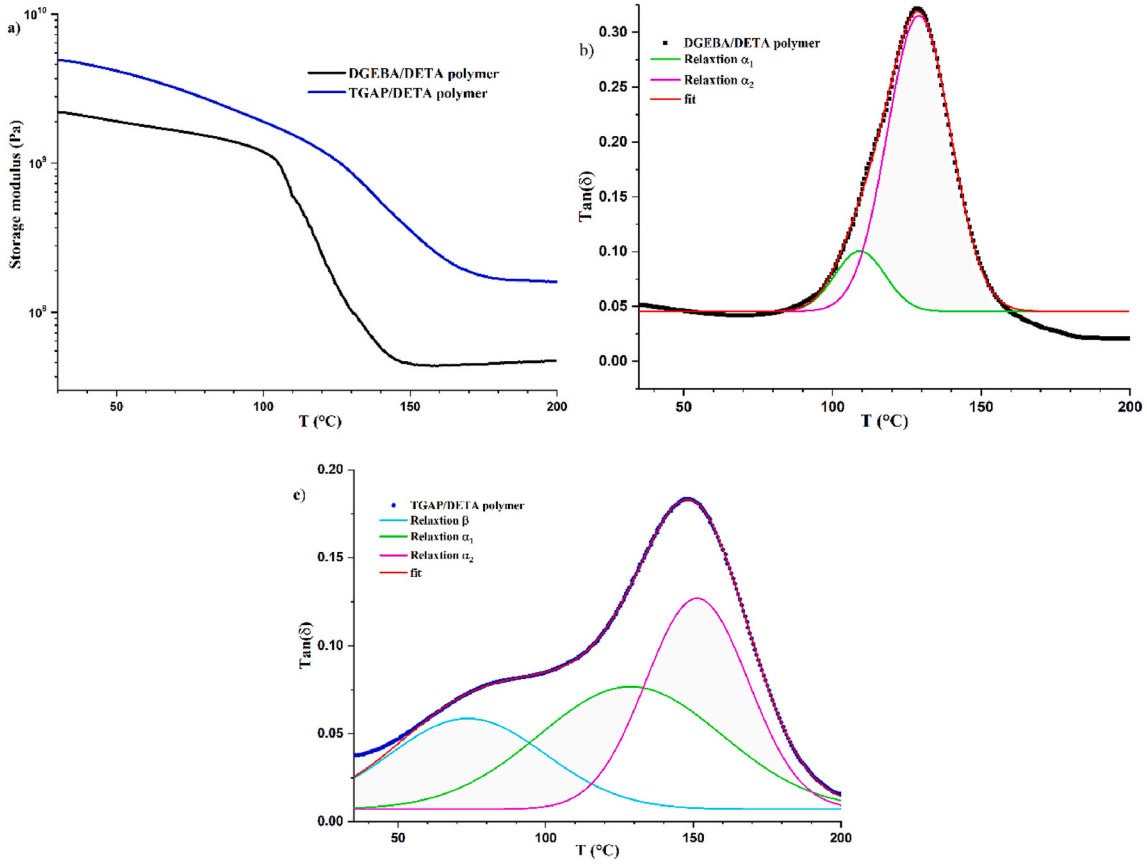

Fig. 8. Dynamic mechanical analysis for DGEBA/DETA and TGAP/DETA polymers: (**a**) storage modulus variations versus temperature. (**b**) and (**c**) Tan(δ) variations versus temperature and the further deconvolution for DGEBA/DETA and TGAP/DETA, respectively.

Then,

$$\frac{d(Ln(\alpha h\upsilon))}{d\,(h\upsilon)} = \frac{n}{h\upsilon - E_g} \quad (3)$$

The advantage of the derivative, in this case, is to highlight the singularities while allowing a more accurate estimation of the gap, since the derivative will reach its maximum value for photon energy close to E_g. Accordingly, we plotted the variation of Ln (αhν) versus (hν) for both polymers (figures not shown here), then we numerically differentiated the obtained plots. The corresponding graphs are presented in Fig. 7.

As expected, the derivative function (Fig. 7a) presented an extremum around 4.098 eV, ascribed to E_g value for DGEBA/DETA polymer. Considering only energies higher than Eg, the curve can be perfectly fitted by a power law of: $\frac{a}{h\upsilon - b}$

The fit parameters were $a = 0.082 \pm 0.013$ and $b = (4.102 \pm 0.002)$ eV. The value of a is far from that of 0.5 expected for direct transition, whereas b is the same (within uncertainties) as E_g value.

For TGAP/DETA polymer, the derivative function (Fig. 7b) presents two close peaks: a maximum around 3.365 eV and a local extremum at about 3.488 eV. The presence of two peaks, and not only one as in the case of DGEBA/DETA, confirms the hypothesis of an indirect transition. Indeed, this one takes place only when supported by phonons [47], which leads to a slight change in eq. (1):

$$\alpha h\upsilon = A\left[h\upsilon - \left(E_g \pm E_p\right)\right]^n \text{ for } h\upsilon > \left(E_g \pm E_p\right) \quad (4)$$

where E_p is the energy of the absorbed or emitted phonon; (E_g - E_p) in case of absorption and ($E_g + E_p$) in case of emission.

Thus, we can ascribe the energies of 3.365 eV and 3.488 eV to (E_g – E_p) and (E_g + E_p) respectively. This means that the indirect optical bandgap is of 3427 eV and the phonon energy is of order of 61.5 meV. By using the same power law, as for DGEBA/DETA, the two characteristic regions can be fitted separately. The adjustment parameters were $a = 0.262 \pm 0.011$ and $b = (3.343 \pm 0.001)$ eV for the first peak, and $a = 0.167 \pm 0.012$ and $b = (3.413 \pm 0.006)$ eV. The values of b extracted from the fit are the same as those determined from extrema, with uncertainties of less than 1% and 2% for the first and the second extrema, respectively. As for the value of a, here again it is far from that of 2 expected for indirect transition. Nevertheless, considering the ratios of the exponents, *i.e.*, 2/0.5 and 0.262/0.083, the relative deviation does not exceed 20%, which is acceptable, pondering the different causes of error and the different phenomena contributing to absorption that are not considered in the approach using the Tauc's relationship. Of course, this pathway should be verified on other materials in future studies to validate it and to elucidate the causes behind the observed discrepancy.

The other advantage of the derivative approach is that of highlighting certain singularities which are difficult or even impossible to observe in the original spectra at energies lower than the optical bandgap. In the present case, the peaks observed at 2.59 eV (479 nm) and 2.93 eV (423 nm) indicate that localized optical transitions can take place, as for semiconductors for which localized disorder may introduce energy levels in the bandgap. The existence of nanostructures within the amorphous matrix of TGAP/DETA, as revealed by XRD measurements, is probably at the origin of absorption in the violet-bleu region (380–490 nm). This property resulted in slightly yellowish coloring of the polymer samples.

The observed differences between the two studied polymers should be emphasized by dielectric investigations, in terms of conductivity and/or relaxations.

3.3. Dynamic mechanical thermal analysis

Dynamic Mechanical Thermal Analysis (DMTA) was investigated to follow up the viscoelastic properties of the synthesized polymers. The variations of storage modulus versus the heating temperatures are illustrated in Fig. 8a. It can be noticed that the storage modulus of the TGAP/DETA polymer is three times superior to that of DGEBA/DETA polymer. This may be due to the higher crosslinking degree of TGAP/DETA polymer, as TGAP possesses 3 epoxy functional groups, while DGEBA has only 2. The network density is therefore higher for TGAP than for DGEBA. This allows a greater degree of stress transfer and consequently leads to an improvement in rigidity [40].

A further temperatures' increase beyond the glass transition region induces a sharp decrease in the value of the storage modulus, which is attributed to an increase in the mobility of both polymers' chains.

Fig. 8b and c presents the dissipation factor as a function of temperature for both polymers. The large and asymmetric shape of the tan (δ) peaks suggests the presence of more than one relaxation for DGEBA/DETA and TGAP/DETA. Moreover, the appearance, at lower temperatures, of another peak in the TGAP/DETA suggests the presence of a third relaxation for this polymer.

The deconvolution of the tan(δ) curves with gaussian functions permitted to obtain individual relaxation peaks, and thus to estimate the relaxation temperatures. The corresponding values are gathered in Table 2.

The deconvolution of the tan(δ) curves, in the glass transition zone, was made in two peaks for both polymers [42,43]. The first one, $T_{\alpha 1}$, is attributed to the transition of the long chains between the crosslinking nodes. $T_{\alpha 1}$ values were of order of 109.5 °C and 129 °C for DGEBA/DETA and TGAP/DETA, respectively. The second peaks, $T_{\alpha 2}$, can be assigned to the motion of the short chains in the most rigid phase [41]. $T_{\alpha 2}$ values were of order of 128.8 °C and 151.3 °C for DGEBA/DETA and TGAP/DETA, respectively. The fact that $T_{\alpha 1}$ and $T_{\alpha 2}$ values of TGAP/DETA are higher than those of DGEBA/DETA confirms that the former has a higher network connectivity than the latter. The third relaxation peak, around 73.6 °C, present in the TGAP/DETA DMTA spectra (Fig. 8c) can be attributed to the β relaxation, which was not observable for the DGEBA/DETA polymer.

Table 2
Relaxation temperatures estimated from the deconvolution of tan(δ) curves with gaussian functions.

Polymer	Relaxation	Temperature (°C)
DGEBA/DETA	α1	109.5
	α2	129
TGAP/DETA	β	73.6
	α1	128.8
	α2	151.3

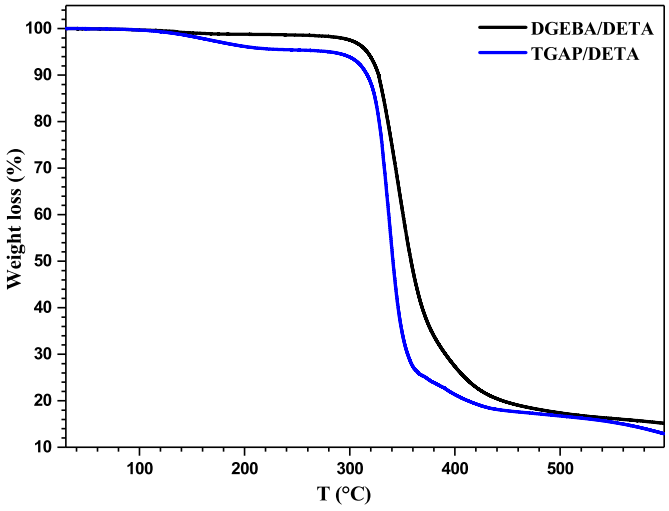

Fig. 9. Weight loss of DGEBA/DETA and TGAP/DETA polymers versus temperature.

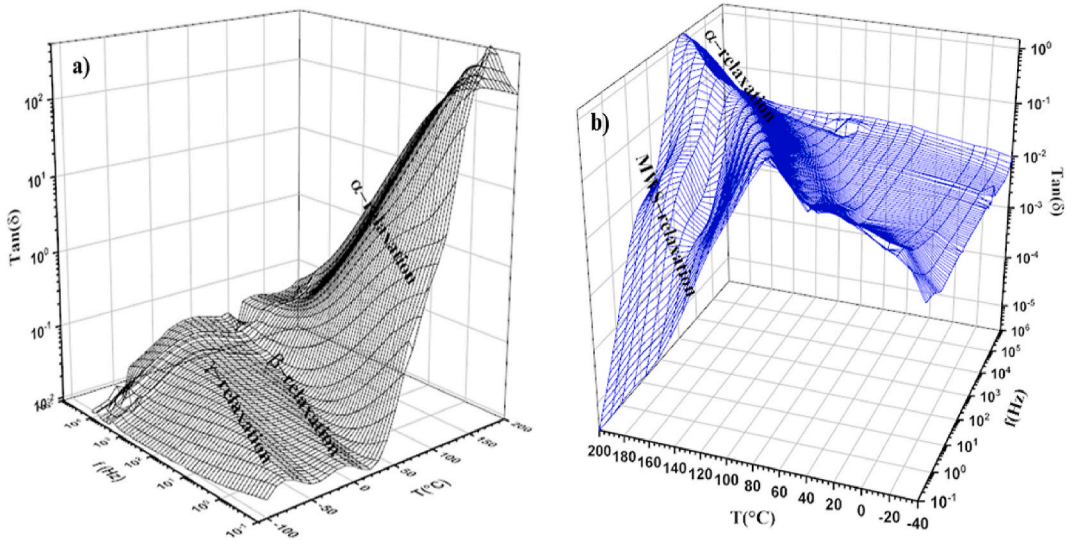

Fig. 10. Dissipation factor versus frequency at various temperatures for (**a**) DGEBA/DETA and (**b**) TGAP/DETA polymers. For better visibility, different view-sides have been adopted for the two representations.

3.4. Thermal stability

The thermograms (Fig. 9) obtained during the TGA scans, for both DGEBA/DETA and TGAP/DETA polymers, were analyzed to estimate the weight losses' percentages as a function of temperature.

Fig. 9 shows an initial slight loss in weight, caused by the evaporation of water molecules, at about 180 °C for DGEBA/DETA and 230 °C for TGAP/DETA. The fact that the percentage of weight loss for TGAP/DETA (≈4.5%) is higher than that of DGEBA/DETA (≈1.2%) can be attributed to the presence of water molecules trapped in the polymeric matrix of TGAP/DETA polymer. This hypothesis is confirmed by the FTIR analysis, as the υ (O–H) absorption band is more intense in the TGAP/DETA polymer than in the DGEBA/DETA one.

This first step was followed by a sharp break, from 310 °C to 485 °C, in both thermograms indicating the onset of a decomposition process. The decomposition rates decrease after that gradually, reaching a constant weight loss of about 82.7% for both TGAP/DETA and DGEBA/DETA polymers, which represents the carbonized char.

3.5. Dielectric characterization

The dielectric responses of DGEBA/DETA and TGAP/DETA polymers, in terms of variations of the tan(δ) dissipation factor versus frequency for different temperatures, are depicted in Fig. 10.

Fig. 10a highlights the existence of three relaxations for the DGEBA/DETA polymer. The first one is γ relaxation which is active at low temperatures: its value varies from about −63 °C for low frequencies to about 0 °C for the high frequencies. Several authors have linked this relaxation to the movement of the diphenyl propane group, or to the rotation of either the methylene sequence or the hydroxy-ether group [28,42,43]. The second relaxation, the β one, can be attributed to the twisting of the hydroxyl and/or carbonyl side groups or to a crankshaft type movement of the hydroxy-ether group in association with the friction movement without rotation of the segments containing the benzene rings [43–45]. For the investigated DGEBA/DETA polymer, the β relaxation provides a small contribution to relaxation processes and is active from 0 °C for low frequencies to about 50 °C for the high ones. γ and β are the secondary relaxations as they are linked to restricted local motions of the polymer chains [50].

The third and main relaxation is the α one which is generally close to the glass transition temperature (Tg) and which is related to the segmental dynamics of the main polymer chains [48,49,51]. Here also α values move towards higher temperatures with increasing frequencies.

Contrarily to DGEBA/DETA polymer, the TGAP/DETA one does not have secondary γ and β relaxations but a Maxwell-Wagner-Sillars (MWS) one, which appears at high temperatures (Fig. 10b). This relaxation is attributed to the accumulation of charges at the interfaces in heterogeneous medium [51–53]. This result is in phase with the XRD ones, concerning the existence of localized nanostructures.

Compared to DMTA results, we note the absence of β relaxation in the TGAP/DETA polymer and the absence of α_1 relaxation in both TGAP/DETA and DGEBA/DETA polymers. This can happen when several phenomena exist simultaneously but are partially or totally masked because of the predominance of one of them (mainly conduction).

To overcome this difficulty, we considered the electric modulus formalism, as it permits to minimize the conduction effects, highlighting thus the relaxations phenomena. The variations of the real and imaginary parts of the electric modulus, as a function of frequency at different temperatures, for the DGEBA/DETA and TGAP/DETA polymers are presented in Fig. 11.

For all the measurements relating to the DGEBA/DETA polymer, we have fit the data with the Havriliak-Negami model according to equation (5) [51,54].

$$M^{*} = M_{\infty} M_s \frac{[(M_{\infty} - M_s)\sin\beta\phi]A^{\beta}}{M_s^2 A^{2\beta} + 2A^{\beta}(M_{\infty} - M_s)M_s \cos\beta\phi + (M_{\infty} - M_s)^2} \tag{5}$$

Where:

$$M_s = \frac{1}{\varepsilon_s},\ M_{\infty} = \frac{1}{\varepsilon_{\infty}},\ A = \left[1 + 2(\omega\tau)^{1-\alpha}\sin\frac{\pi\alpha}{2} + (\omega\tau)^{2(1-\alpha)}\right]^{\frac{1}{2}};$$

$$\phi = arctg\left[\frac{(\omega\tau)^{1-\alpha}\cos\frac{\pi\alpha}{2}}{1 + (\omega\tau)^{1-\alpha}\sin\frac{\pi\alpha}{2}}\right];$$

ε_s and ε_{∞} are, respectively, the dielectric constants for the low- and high-frequency sides of relaxation, β and α are, respectively, the parameters describing the asymmetric and symmetric broadening of the relaxation time and τ is the central relaxation time.

We were however not been able to the TGAP/DETA experimental data with this model.

According to the electrical modulus variations, we can conclude that the α_2 relaxation observed by DMTA corresponds to a weak depolarization for DGEBA/DETA and to predominant conduction effect for TGAP/DETA. Therefore, it is useful to consider conductivity of both

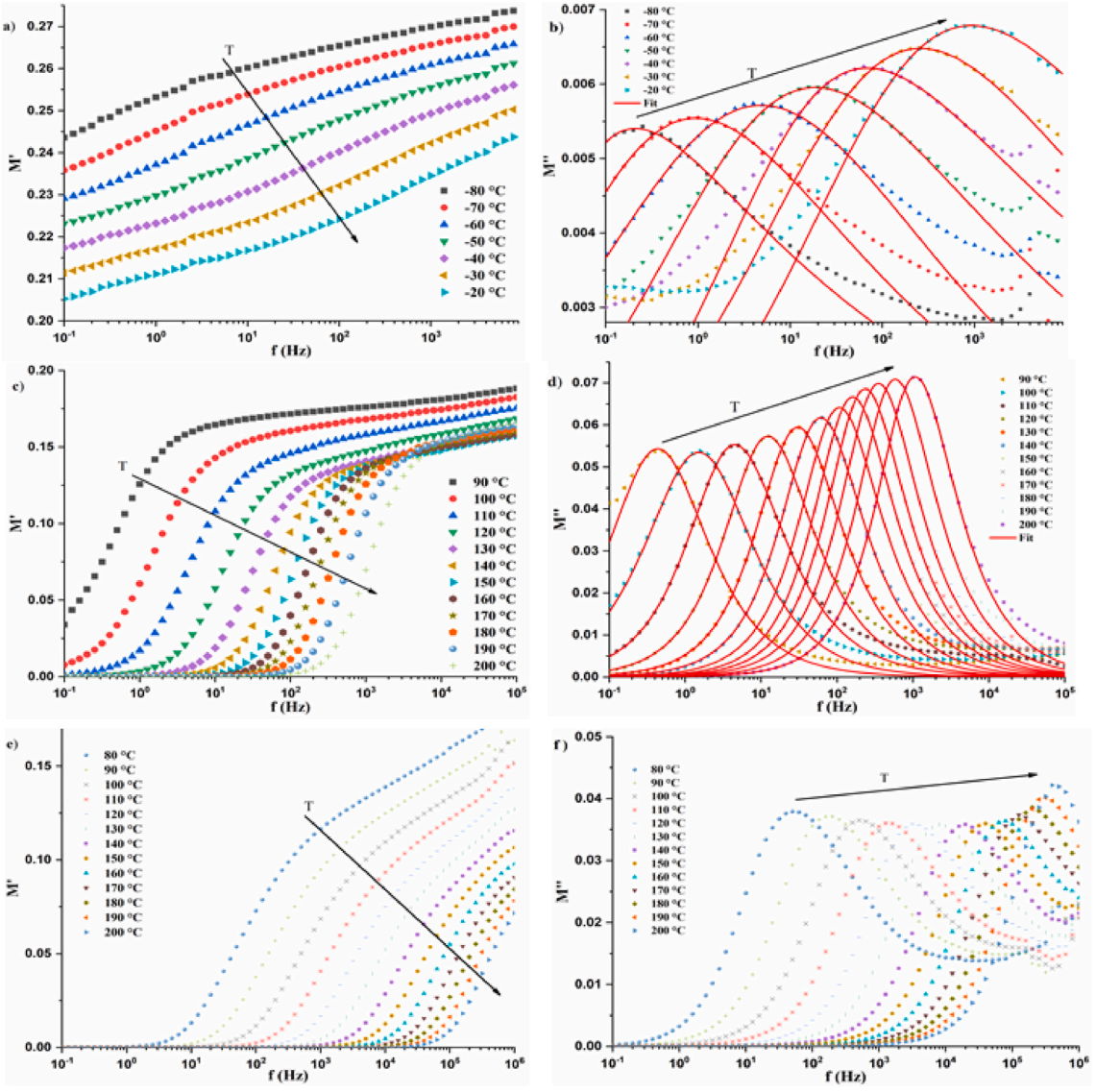

Fig. 11. Electric Modulus versus frequency at various temperatures for (**a**, **b**, **c** and **d**) DGEBA/DETA polymer and (**e** and **f**) TGAP/DETA polymer.

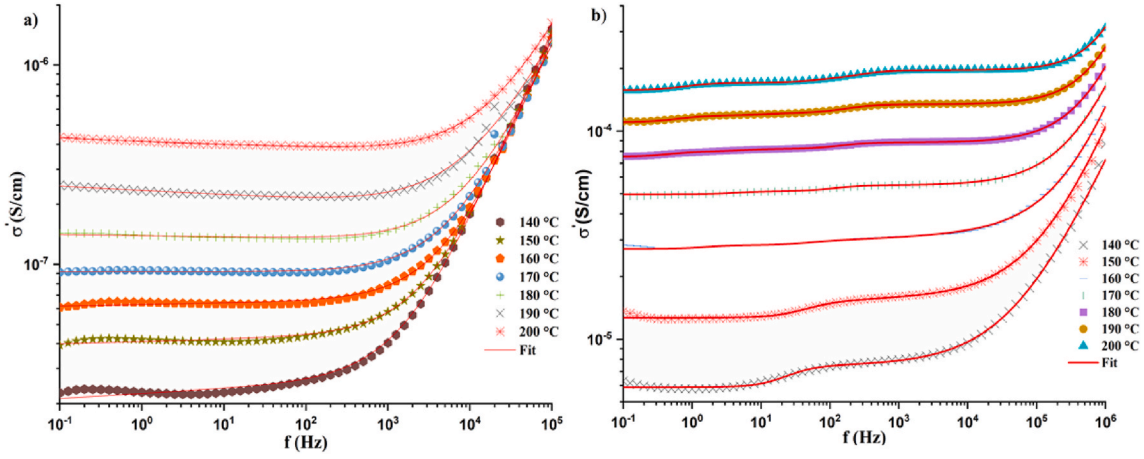

Fig. 12. Conductivity versus frequency at various temperatures for (**a**) DGEBA/DETA polymer and (**b**) TGAP/DETA polymer.

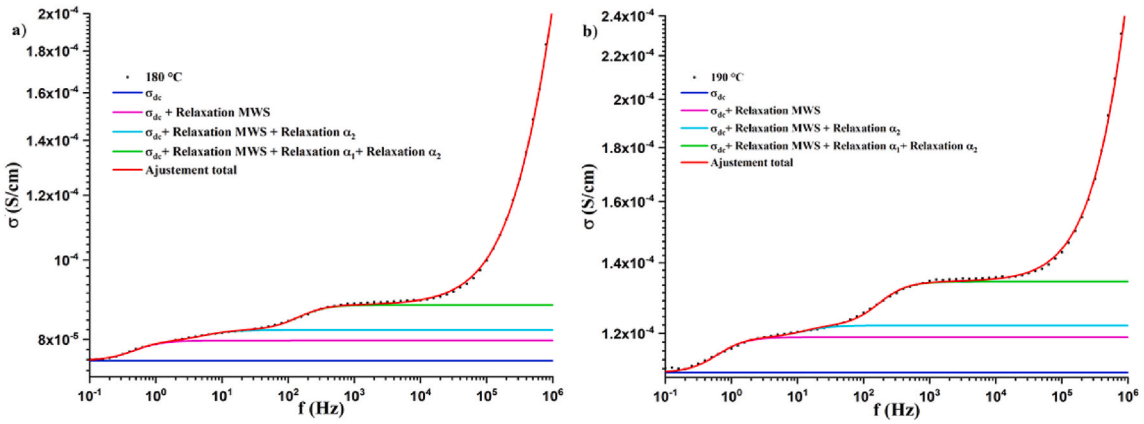

Fig. 13. Conductivity of TGAP/DETA versus frequency (a) at 180C; (b) at 190 °C.

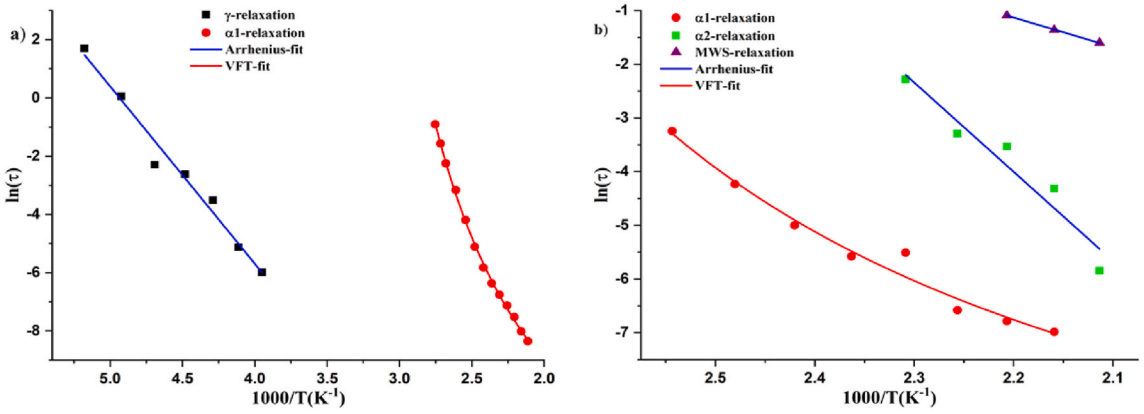

Fig. 14. Variation of the relaxation times versus 1000/T for (a) DGEBA/DETA polymer and (b) TGAP/DETA polymer.

polymers according to the following equation:

$$\sigma'(w) = \sigma_{dc} + \varepsilon_0 \omega \sum_{i=1}^{n} \left(\frac{(\varepsilon_s - \varepsilon_\infty)_i * \sin(\theta_i)}{\left(1 + (w\tau_i)^{2\alpha_i} + 2(w\tau_i)^{\alpha_i} * \cos\left(\frac{\alpha_i * \pi}{2}\right)\right)^{\frac{\beta_i}{2}}} \right) + A\omega^s \qquad (6)$$

Where: $\theta_i = \text{arctg}\left[\frac{(\omega\tau_i)^{(1-\alpha_i)} * \cos\left(\frac{\pi * \alpha_i}{2}\right)}{1 + (\omega\tau_i)^{(1-\alpha_i)} * \sin\left(\frac{\pi * \alpha_i}{2}\right)}\right]$,

i is the index corresponding of each identified relaxation, n is their total number, ω is the angular frequency, A is a constant, s is an exponent of the angular frequency and σ_{dc} is the limit value of σ' (ω → 0). The variations of the DGEBA/DETA and TGAP/DETA conductivities as a function of frequency at different temperatures are presented in Fig. 12.

These results showed that the TGAP/DETA conductivity is about two orders of magnitude higher than that of DGEBA/DETA, for all the investigated temperatures. This is in phase with optical measurements in terms of estimated bandgap values and existence of low energy transitions states.

Table 3
Activation energies for the different relaxations observed in DGEBA/DETA and TGAP/DETA polymers.

Polymers	γ	MWS	α1	α2
DGEBA/ DETA	0.5 eV/ 48.07 kJ/ mol	–	1.39 eV/ 133.65 kJ/mol	–
TGAP/ DETA	–	0.43 eV/ 41.34 kJ/mol	1.32 eV/ 126.92 kJ/mol	1.24 eV/ 119.23 kJ/mol

To minimize the scale effect and to have an enlarged view, we considered separately the conductivity measurements of TGAP/DETA at 180 °C (Fig. 13a) and at 190 °C (Fig. 13b). At these temperatures, the cumulative effects of all involved phenomena are clearly identified.

By using an appropriate adjustment model, we showed that is possible to identify each contribution to conductivity, not only MWS relaxation phenomenon but also α_1 and α_2 relaxation ones, as observed in the DMTA analysis.

Using τ and σ_{dc} parameters determined by the adjustment of the electrical modulus and the conductivity, we can calculate the activation energy of the relaxations and the conductivity. In Fig. 14, we plotted ln (τ) versus 1000/T for DGEBA/DETA and TGAP/DETA polymers.

The plots corresponding to γ relaxation in DGEBA/DETA and the α_2 and MWS relaxations in TGAP/DETA exhibit a linear behavior which was fitted according to Arrhenius equation [50]:

$$\tau(T) = \tau_0 \exp\left(\frac{E_a}{K_B T}\right) \qquad (7)$$

Where K_B is the Boltzmann constant, E_a is the activation energy of the relaxation process and T is the absolute temperature.

α_1 relaxation, in both DGEBA/DETA and TGAP/DETA, polymers was fitted by the Vogel–Fulcher–Tammann (VFT) model, which was found more appropriate than the Arrhenius one. Its further equation is [52]:

$$\tau(T) = \tau_0 \exp\left(\frac{B}{T_V - T}\right) \qquad (8)$$

T_V is the Vogel temperature and B is an empirical material-dependent parameter, which permits to calculate the further activation energy, E_a, from the equation:

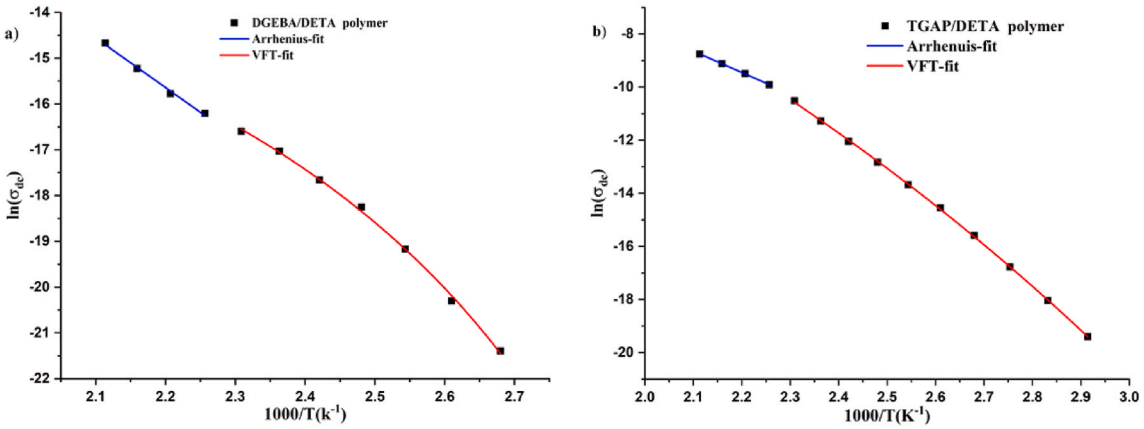

Fig. 15. Temperature dependence of the dc conductivity for (a) DGEBA/DETA and (b) TGAP/DETA polymers.

Table 4
σ_{dc} activation energies of for DGEBA/DETA and TGAP/DETA polymers.

		DGEBA	TGAP
VFT model	130 °C	1.06 eV/101.92 kJ/mol	1.16 eV/111.53 kJ/mol
	140 °C	0.94 eV/90.83 kJ/mol	1.13 eV/108.65 kJ/mol
	150 °C	0.84 eV/80.76 kJ/mol	1.09 eV/104.8 kJ/mol
	160 °C	0.76 eV/73.07 kJ/mol	1.06 eV/101.92 kJ/mol
Arrhenius model	160–200 °C	0.62 eV/59.61 kJ/mol	0.62 eV/59.61 kJ/mol

$$E_a = \frac{RB}{\left(1 - \frac{T_v}{T_g}\right)^2} \quad (9)$$

Where R is the gas constant and T_g is the glass transition temperature.

The values of the activation energies of the relaxations are gathered in Table 3.

The Vogel–Fulcher–Tammann (VFT) dependence on temperature is the typical signature of the α_1 relaxation, which is the dielectric manifestation of the glass transition which involves the cooperative mobility of the polymer network [28].

It can be noted that the activation energy value for the α_1 relaxation in DGEBA/DETA is superior to that of TGAP/DETA. This can be linked to molecular chain mobility [28].

The last part of this study concerns to the variations of dc conductivity, σ_{dc}, of DGEBA/DETA and TGAP/DETA polymers. Fig. 15 represents the variations of ln (σ_{dc}) versus 1000/T.

Results presented in Fig. 15 show the presence of two behaviors that depend on the temperature domain: a linear one (following the Arrhenius law) for temperatures higher than 160 °C and a nonlinear one (following the VFT model) for lower temperatures. For this last case, σ_{dc} activation energies were calculated from eq (10). The computed values are given in Table 4.

Calculations indicate that the σ_{dc} activation energies are identical for both polymers at temperatures higher than 160 °C, and that those of DGEBA are lower than those of TGAP ones at temperatures inferior to 160 °C. On the basis of these results, we can suppose that the conduction is ionic for "low" temperatures and that it is dominated by the movement of polymer chains at "high" ones. The fact that the activation energy of the TGAP/DETA polymer is higher than that of the DGEBA/DETA polymer, can be attributed to the high degree of crosslinking of the TGAP polymer, which rends it is more rigid than the DGEBA [53].

4. Conclusion

This study focuses on the comparison of structural, optical, dynamic mechanical, thermal properties of the TGAP/DETA and DGEBA/DETA polymers. The results have shown that the two polymers have good thermal stability and present an amorphous character. Both polymers exhibit excellent transparency in the visible light. However, the TGAP polymer, absorbs almost completely UV radiations and partially blue-violet light which explains its slightly yellowish coloring. Absorption peaks observed around 2.59 eV and 2.93 eV (wavelengths of order of 479 nm and 423 nm respectively) indicate that localized optical transitions take place from energy levels in the bandgap. This was ascribed to the existence of nanostructures within the amorphous matrix of TGAP/DETA, as revealed by XRD measurements. This polymer has shown sufficiently interesting mechanical and optical properties to be considered in applications as a protective film and/or as a UV/blue light filter for screens and windows. The difference between the two polymers also concerns their optical bandgap energy of about 3.4 eV and 4.1 eV for TGAP and DGEBA, respectively. For a more accurate estimation of Eg value and to better account for the nature of the transition in studied polymers, a novel approach of results processing is proposed based on the logarithmic derivative of Tauc's law. The dielectric measurements indicated the presence of γ, β, α_1 and α_2 dipolar relaxations and MWS interfacial one. The latter, observed only in the case of TGAP, is again consistent with the presence of crystalline micro-zones within the amorphous matrix. Experimental data of the electrical modulus and the conductivity were analyzed according to the Havriliak-Negami approach. The relaxation times and the conductivity σ_{dc} were investigated using Arrhenius and VFT models. For high temperatures (above 160 °C), where the ionic conduction is dominant, Arrhenius behavior was observed for both polymers with the same activation energy. For all temperatures below 160 °C, the non-linear behavior was approached by the VFT model for both polymers, and the activation energies were found to be lower for the DGEBA compared to the TGAP.

Author contributions

Conceptualization and methodology, H.J., N.F., C.Z. and H.G.; optical measurements, H.J. and M.F; dielectric measurements, H.J. and L. I.; mechanical/thermal measurements, H.J. and A.G.; software, investigation and writing—original draft preparation, H.J.; formal analysis and data curation, H.J. and W.J; writing—review and editing, H.J., N.F., C.Z. and H.G.; validation and supervision, H.G. and C.Z.; visualization, N.F., C.Z., H.G. and S.G.; funding acquisition, C.Z., H.G. and S.G.

Funding

This work was partially funded by Campus France and CMCU via the PHC Utique project n°37095 ZF/17G1143 TU.

Declaration of competing interest

The authors declare that they have no known competing financial interests or personal relationships that could have appeared to influence the work reported in this paper.

Acknowledgment

The authors would like to thank Campus France and CMCU committee for the financial support of this work via the PHC Utique project n°37095 ZF/17G1143 TU.

References

[1] S.E. Lee, E. Jeong, M.Y. Lee, M.K. Lee, Y.S. Lee, Improvement of the mechanical and thermal properties of polyethersulfone-modified epoxy composites, J. Ind. Eng. Chem. 33 (2016) 73–79, https://doi.org/10.1016/j.jiec.2015.09.022.

[2] N. Saba, M. Jawaid, O.Y. Alothman, M.T. Paridah, A. Hassan, Recent advances in epoxy resin, natural fiber-reinforced epoxy composites and their applications, J. Reinforc. Plast. Compos. 35 (2016) 447–470, https://doi.org/10.1177/0731684415618459.

[3] O.A. Amariutei, R. Ramsdale-Capper, M. Correa Álvarez, L.K.Y. Chan, J. P. Foreman, Modelling the properties of a difunctional epoxy resin cured with aromatic diamine isomers, Polymer (Guildf) 156 (2018) 203–213, https://doi.org/10.1016/j.polymer.2018.10.016.

[4] G. Cicala, S. Mannino, A. Latteri, G. Ognibene, G. Saccullo, Effects of mixing di- and tri-functional epoxy monomers on epoxy/thermoplastic blends, Adv. Polym. Technol. 37 (2018) 1868–1877, https://doi.org/10.1002/adv.21845.

[5] M. El Dagdag, O. Azzouz, E. Gana, L. El Bouchti, A. Othman, H. Cherkaoui, O. Shehdeh, J. El Harfi, Synthesis, characterization and rheological properties of epoxy monomers derived from bifunctional aromatic amines, Polym. Bull. 76 (9) (2018) 4399–4413, https://doi.org/10.1007/s00289-018-2607-4.

[6] C.N. Cas, D. Ros, F. Mustat, Investigation of the curing reactions of some multifunctional epoxy resins using differential scanning calorimetry, Thermochim. Acta 370 (2001) 105–110.

[7] D. Ros, C.N. Cas, F. Mustat, C. Ciobanu, Cure Kinetics of epoxy resines studied by non-isothermal DSC data, Thermochim. Acta 383 (2002) 119–127.

[8] B. Francis, Cure kinetics of epoxy/thermoplastic blends, Handb. Epoxy Blends (2017) 1–1121, https://doi.org/10.1007/978-3-319-40043-3.

[9] I. Aazem, A. Kumar, M. Mohapatra, J.H. Cho, J. Joyner, P.S. Owuor, J. Parameswaranpillai, V.K. Thakur, J.J. George, R. Prasanth, Thermal Properties of Epoxy/Thermoplastic Blends, 2017, https://doi.org/10.1007/978-3-319-40043-3.

[10] D. Ratna, Handbook of Thermoset Resins, 2009, https://doi.org/10.1002/0471743984.vse3011.pub2.

[11] A. Romo-Uribe, Dynamic Mechanical Thermal Analysis of Epoxy/Thermoplastic Blends, 2017, https://doi.org/10.1007/978-3-319-40043-3.

[12] N.M. Florea, A. Lungu, P. Badica, L. Craciun, M. Enculescu, D.G. Ghita, C. Ionescu, R.G. Zgirian, H. Iovu, Novel nanocomposites based on epoxy resin/epoxy-functionalized polydimethylsiloxane reinforced with POSS, Compos. B Eng. 75 (2015) 226–234, https://doi.org/10.1016/j.compositesb.2015.01.043.

[13] D. dong Hu, J. xun Lyu, T. Liu, M. dong Lang, L. Zhao, Solvation effect of CO2 on accelerating the curing reaction process of epoxy resin, Chem. Eng. Process. - Process Intensif. 127 (2018) 159–167, https://doi.org/10.1016/j.cep.2018.01.027.

[14] M. Korey, G.P. Mendis, J.P. Youngblood, J.A. Howarter, Tannic acid: a sustainable crosslinking agent for high glass transition epoxy materials, J. Polym. Sci. Part A Polym. Chem. 56 (2018) 1468–1480, https://doi.org/10.1002/pola.29028.

[15] R. Li, W. Li, F. Zheng, Y. Zhang, J. Hu, Versatile bio-based epoxy resin: from banana waste to applied materials, J. Appl. Polym. Sci. 136 (2019) 1–8, https://doi.org/10.1002/app.47135.

[16] T.M. Lee, C.C.M. Ma, C.W. Hsu, H.L. Wu, Syntheses of epoxy-bridged polyorganosiloxanes and the effects of terminated alkoxysilanes on cured thermal properties, J. Appl. Polym. Sci. 99 (2006) 3491–3499, https://doi.org/10.1002/app.22973.

[17] J.Y. Shieh, C.S. Wang, Effect of the organophosphate structure on the physical and flame-retardant properties of an epoxy resin, J. Polym. Sci. Part A Polym. Chem. 40 (2002) 369–378, https://doi.org/10.1002/pola.10121.

[18] H. Behniafar, S. Haghighat, Thermally stable and organosoluble binaphthylene-based poly(urea-ether-imide)s: one-pot preparation and characterization, Polym. Adv. Technol. 19 (2008) 1040–1047, https://doi.org/10.1002/pat.

[19] K.P. Unnikrishnan, E.T. Thachil, Aging and thermal studies on epoxy resin modified by epoxidized novolacs, Polym. Plast. Technol. Eng. 45 (2006) 469–474, https://doi.org/10.1080/03602550600553762.

[20] Z. Yang, H. Peng, W. Wang, T. Liu, Crystallization behavior of poly (ε-caprolactone)/layered double hydroxide nanocomposites, J. Appl. Polym. Sci. 116 (2010) 2658–2667, https://doi.org/10.1002/app.

[21] P. Czub, Synthesis and modification of epoxy resins using recycled poly(ethylene terephthalate), Polym. Adv. Technol. 20 (2009) 183–193, https://doi.org/10.1002/pat.1251.

[22] F. Ferdosian, Z. Yuan, M. Anderson, C. Xu, Sustainable lignin-based epoxy resins cured with aromatic and aliphatic amine curing agents: curing kinetics and thermal properties, Thermochim. Acta 618 (2015) 48–55, https://doi.org/10.1016/j.tca.2015.09.012.

[23] G. Ognibene, S. Mannino, M.E. Fragalà, G. Cicala, Trifunctional epoxy resin composites modified by soluble electrospun veils: effect on the viscoelastic and morphological properties, Materials 11 (2018), https://doi.org/10.3390/ma11030405.

[24] J.M. H, Y.C. Fatemeh Shiravand, A novel comparative study of different layered silicate clay types on exfoliation process and final nanostructure of trifunctional epoxy nanocomposites, Polym. Test. 56 (2016) 148–155.

[25] J.M. Hutchinson, F. Shiravand, Y. Calventus, I. Fraga, Isothermal and non-isothermal cure of a tri-functional epoxy resin (TGAP): a stochastic TMDSC study, Thermochim. Acta 529 (2012) 14–21, https://doi.org/10.1016/j.tca.2011.11.008.

[26] N. Bai, G.P. Simon, K. Saito, Characterisation of the thermal self-healing of a high crosslink density epoxy thermoset, New J. Chem. 39 (2015) 3497–3506, https://doi.org/10.1039/c5nj00066a.

[27] J. Hu, J. Shan, J. Zhao, Z. Tong, Isothermal curing kinetics of a flame retardant epoxy resin containing DOPO investigated by DSC and rheology, Thermochim. Acta 632 (2016) 56–63, https://doi.org/10.1016/j.tca.2016.02.010.

[28] W. Jilani, N. Mzabi, N. Fourati, C. Zerrouki, O. Gallot-Lavallée, R. Zerrouki, H. Guermazi, A comparative study of structural and dielectric properties of diglycidyl ether of bisphenol A (DGEBA) cured with aromatic or aliphatic hardeners, J. Mater. Sci. 51 (2016) 7874–7886, https://doi.org/10.1007/s10853-016-0043-0.

[29] Ehsan Moaseri, B. Bazubandi, M. Karimi, M. Maghrebi, M. Baniadam, Mechanical improvements of multi-walled carbon nanotube-epoxy composite: covalent functionalization of multi-walled carbon nanotube by epoxy chains, Polym. Sci. B 61 (2019) 341–348, https://doi.org/10.1134/S1560090419030072.

[30] J. Tauc, Amorphous and Liquid Semiconductor, Plenum, New York, 1974, p. 159.

[31] R. Pal, S. Sudhi, R. Raghavan, Fabrication and evaluation of structural film adhesive using oxazolidinone modified novolac epoxy resin, J. Appl. Polym. Sci. 136 (2019) 1–10, https://doi.org/10.1002/app.47520.

[32] Hariharan Nhalil, Dan Han, Mao-Hua Du, Shiyou Chen, Daniel Antonio, Krzysztof Gofryk, Bayrammurad Saparov, Optoelectronic properties of candidate photovoltaic Cu2PbSiS4, Ag2PbGeS4 and KAg2SbS4 semiconductors, J. Alloys Compd. 746 (2018), 405e412, https://doi.org/10.1016/j.jallcom.2018.02.331.

[33] Rashmi Chauhan, Determination of optical transition nature using R2 value, Int. Arch. App. Sci. Technol 6 (3) (2015) 28–30, https://doi.org/10.15515/iaast.0976-4828.6.3.2830.

[34] Santosh K. Suram, Paul F. Newhouse, John M. Gregoire, High throughput light absorber discovery, Part 1: an algorithm for automated Tauc analysis, ACS Comb. Sci. 18 (2016) 673–681, https://doi.org/10.1021/acscombsci.6b00053.

[35] D.V. Likhachev, N. Malkova, L. Poslavsky, Modified Tauc–Lorentz dispersion model leading to a more accurate representation of absorption features below the bandgap, Thin Solid Films 589 (2015) 844–851, https://doi.org/10.1016/j.tsf.2015.07.035.

[36] Y. Feng, C. He, Y. Wen, Y. Ye, X. Zhou, X. Xie, Y.W. Mai, Improving thermal and flame retardant properties of epoxy resin by functionalized graphene containing phosphorous, nitrogen and silicon elements, Compos. Part A Appl. Sci. Manuf. 103 (2017) 74–83, https://doi.org/10.1016/j.compositesa.2017.09.014.

[37] X. Zhao, Q. Zhang, D. Chen, P. Lu, Enhanced mechanical properties of graphene-based polyvinyl alcohol composites, Macromolecules 43 (2010) 2357–2363, https://doi.org/10.1021/ma902862u.

[38] M. Dresselhaus, Solid state physics Part I - transport properties of solids, Lect. Notes. (1999) 233.

[39] N. Hameed, P.A. Sreekumar, B. Francis, W. Yang, S. Thomas, Morphology, dynamic mechanical and thermal studies on poly(styrene-co-acrylonitrile) modified epoxy resin/glass fibre composites, Compos. Part A Appl. Sci. Manuf. 38 (2007) 2422–2432, https://doi.org/10.1016/j.compositesa.2007.08.009.

[40] D.K. Chouhan, A. Kumar, S.K. Rath, S. Kumar, P.S. Alegaonkar, G. Harikrishnan, T. Umasankar Patro, Laponite-graphene oxide hybrid particulate filler enhances mechanical properties of cross-linked epoxy, J. Polym. Res. 25 (2018), https://doi.org/10.1007/s10965-018-1461-2.

[41] S. Pangrle, C.S. Wu, P.H. Geil, Low temperature relaxation of DGEBA epoxy resins: a thermally stimulated discharge current (TSDC) study, Polym. Compos. 10 (1989) 173–183, https://doi.org/10.1002/pc.750100305.

[42] I. Erukhimovich, M.O. de la Cruz, Phase Equilibria and Charge Fractionation in Polydisperse Polyelectrolyte Solutions, 2004, pp. 11–17, https://doi.org/10.1002/polb.

[43] G.A. Pogany, Gamma relaxation in epoxy resins and related polymers, Polymer 11 (1970) 66–78, https://doi.org/10.1016/0032-3861(70)90027-3.

[44] R.G.C. Arridge, J.H. Speake, Mechanical relaxation studies of the cure of epoxy resins: 2. Activation energy of the γ-process in amine-cured epoxy resins, Polymer (Guildf). 13 (1972) 450–454, https://doi.org/10.1016/0032-3861(72)90112-7.

[45] Y. Wang, S. Lany, J. Ghanbaja, Y. Fagot-Revurat, Y.P. Chen, F. Soldera, D. Horwat, F. Mücklich, J.F. Pierson, Electronic structures of C u2 O, C u4 O3, and CuO: a joint experimental and theoretical study, Phys. Rev. B 94 (2016), https://doi.org/10.1103/PhysRevB.94.245418.

[46] W. Jilani, N. Mzabi, N. Fourati, C. Zerrouki, O. Gallot-Lavallée, R. Zerrouki, H. Guermazi, Effects of curing agent on conductivity, structural and dielectric properties of an epoxy polymer, Polymer 79 (2015) 73–81, https://doi.org/10.1016/j.polymer.2015.09.078.
[47] A.E. Kraulis, A.T. Echtermeyer, Mechanism of yellowing: carbonyl formation during hygrothermal aging in a common amin epoxy, Polymers 10 (2018) 1017, https://doi.org/10.3390/polym10091017.
[48] A.R. Zanatta, Revisiting the optical bandgap of semiconductors and the proposal of a unified methodology to its determination, Sci. Rep. 9 (2019) 11225, https://doi.org/10.1038/s41598-019-47670-y.
[49] W. Jilani, N. Mzabi, O. Gallot-Lavallée, N. Fourati, C. Zerrouki, R. Zerrouki, H. Guermazi, Dielectric relaxations investigation of a synthesized epoxy resin polymer, Eur. Phys. J. Plus. 130 (2015) 1–10, https://doi.org/10.1140/epjp/i2015-15076-6.
[50] G.A. Kontos, A.L. Soulintzis, P.K. Karahaliou, G.C. Psarras, S.N. Georga, C. A. Krontiras, M.N. Pisanias, Electrical relaxation dynamics in TiO2 - polymer matrix composites, Express Polym. Lett. 1 (2007) 781–789, https://doi.org/10.3144/expresspolymlett.2007.108.
[51] O. Gallot-Lavallée, H. Guermazi, N. Fourati, C. Zerrouki, W. Jilani, Optical, dielectric properties and energy storage efficiency of ZnO/epoxy nanocomposites, 0, J. Inorg. Organomet. Polym. Mater. (2019), https://doi.org/10.1007/s10904-018-1016-3, 0.
[52] H. Hammami, M. Arous, M. Lagache, A. Kallel, Experimental Study of Relaxations in Unidirectional Piezoelectric Composites, vol. 37, 2006, pp. 1–8, https://doi.org/10.1016/j.compositesa.2005.05.049.
[53] H. Smaoui, M. Arous, H. Guermazi, S. Agnel, A. Toureille, Study of relaxations in epoxy polymer by thermally stimulated depolarization current (TSDC) and dielectric relaxation spectroscopy (DRS), J. Alloys Compd. 489 (2010) 429–436, https://doi.org/10.1016/j.jallcom.2009.09.116.
[54] G. Floudas, Dielectric Spectroscopy, Elsevier B.V., 2012, https://doi.org/10.1016/B978-0-444-53349-4.00057-1.